Electronic Supplementary Material (ESI) for Dalton Transactions.


# Efficient synthetic route to heterobimetallic trinuclear complexes [Ln-Mn-Ln] and their single molecule magnetic properties

Nurul F. Ghazali,[a] Kuduva R. Vignesh,[b] Wasinee Phonsri,[a] Zhifang Guo,[a,c] Keith S. Murray,[a]* Peter C. Junk,[c]* Glen B. Deacon,[a]* and David R. Turner [a]*

a. School of Chemistry, Monash University, Clayton, VIC 3800, Australia.

b. Department of Chemical Sciences, IISER Mohali, Sector-81, SAS Nagar, Mohali-140306, Punjab, India.

c. College of Science and Engineering, James Cook University, Townsville, QLD 4811, Australia.

# Supporting Information

1. Crystallographic refinement details
2. Tables of selected bond lengths
3. Magnetic plots
4. PXRD data

## 1. Crystallographic Refinement Details

**1Ln**

Data for the 1Ln series of compounds were all treated using the SQUEEZE routine of PLATON due to areas of diffuse electron density that could not be resolved. In all instances this could be assigned as some combination of water and ethanol, in reasonable agreement with elemental analysis results (allowing for potential solvent exchange or slight sample inhomogeneity with regards to solvation). For refinements, combinations of water and ethanol were used to fit the electron count with the closest integer number of solvent molecules.

Disorder in the tetrabutylammonium cations was treated with a combination of DFIX/DANG restraints and DELU/SIMU as required (see individual CIF files for full information).

**2Ln**

Both **2Tb** and **2Yb** contain partial occupancy chloroform. In **2Yb** this was modelled as a single site with 50% occupancy. Although there is some evidence of a second overlapping position with far smaller occupancy, it could not be modelled. In **2Tb** two sites were modelled with a shared carbon position; these were modelled with fixed occupancies of 50% and 25%, with SADI restraints to give sensible C-Cl distances. In both instances the degree of solvation appears to be slightly less than that calculated through elemental analysis, presumably due to some loss during sample handling.

**3**

No special refinement details.

| | **1Eu** | **1Dy** | **1Ho** | **1Er** | **1Yb** |
|---|---|---|---|---|---|
| **Compound** | $(NBu_4)[Eu(QCl)_4]\cdot EtOH\cdot 2H_2O$ | $(NBu_4)[Dy(QCl)_4]\cdot EtOH\cdot 2H_2O$ | $(NBu_4)[Ho(QCl)_4]\cdot EtOH\cdot 3H_2O$ | $(NBu_4)[Er(QCl)_4]\cdot EtOH\cdot 3H_2O$ | $(NBu_4)[Yb(QCl)_4]\ ]\cdot 2EtOH$ |
| **Empirical formula** | $C_{54}H_{66}Cl_4EuN_5O7$ | $C_{54}H_{66}Cl_4DyN_5O_7$ | $C_{54}H_{68}Cl_4HoN_5O_8$ | $C_{54}H_{68}Cl_4ErN_5O_8$ | $C_{52}H_{56}Cl_4N_5O_4Yb$ |
| **Formula weight** | 1190.87 | 1201.41 | 1221.86 | 1224.19 | 1221.99 |
| **Crystal system** | Monoclinic | Monoclinic | Monoclinic | Monoclinic | Monoclinic |
| **Space group** | $P2_1/c$ | $P2_1/c$ | $P2_1/c$ | $P2_1/c$ | $P2_1/c$ |
| ***a*/Å** | 22.534(5) | 22.599(5) | 22.4676(3) | 22.593(5) | 22.671(5) |
| ***b*/Å** | 22.576(5) | 22.428(5) | 22.5189(2) | 22.512(5) | 22.311(5) |
| ***c*/Å** | 22.796(5) | 22.699(5) | 22.7200(3) | 22.757(5) | 22.597(5) |
| ***α*/°** | - | - | - | - | - |
| ***β*/°** | 107.71(3) | 107.79(3) | 107.882(2) | 107.66(3) | 107.68(3) |
| ***γ*/°** | - | - | - | - | - |
| **Volume/Å³** | 11047(5) | 10955(5) | 10939.8(3) | 11029(5) | 10890(5) |
| **Z** | 8 | 8 | 8 | 8 | 8 |
| **Refs. collected** | 371091 | 128046 | 176620 | 126454 | 162583 |
| **Independent refs.** | 31746 | 19097 | 38081 | 19172 | 23873 |
| **$R_{int}$** | 0.0825 | 0.1058 | 0.0564 | 0.0604 | 0.0767 |
| **GooF** | 1.040 | 1.064 | 1.087- | 1.081 | 1.046 |
| **$R_1$ [I>=2σ (I)/all data]** | 0.0467/0.0638 | 0.0653/0.0929 | 0.0355/0.0603 | 0.0391/0.0404 | 0.0736/0.0997 |
| **$wR_2$ [I>=2σ (I)/all data]** | 0.1253/0.1342 | 0.1619/0.1826 | 0.0764/0.0823 | 0.1127/0.1138 | 0.1835/0.1975 |
| **Diffractometer** | MX1, Australian Synchrotron | MX1, Australian Synchrotron | Rigaku Synergy | Bruker ApexII | MX1, Australian Synchrotron |

**Table S1.** Crystallographic and refinement parameters for the **1Ln** series of compounds.

| | **2Tb** | **2Yb** | **3** |
|---|---|---|---|
| **Compound** | $[Tb_2Mn(QCl)_8]\cdot 0.75CHCl_3$ | $[Yb_2Mn(QCl)_8]\cdot 0.5CHCl_3$ | $[Dy_3(QCl)_8Cl(OH_2)]\cdot 3(Mepy)\cdot H_2O$ |
| **Empirical formula** | $C_{73.5}H_{41.5}Cl_{12.5}MnN_8O_8Tb_2$ | $C_{73}H_{41}Cl_{11}MnN_8O_8Yb_2$ | $C_{90}H_{66}Cl_9Dy_3N_{11}O_{10}$ |
| **Formula weight** | 1980.55 | 1949.11 | 2268.08 |
| **Crystal system** | Triclinic | Triclinic | Monoclinic |
| **Space group** | *P*-1 | *P*-1 | $P2_1/n$ |
| ***a*/Å** | 12.134(2) | 11.983(2) | 14.026(3) |
| ***b*/Å** | 12.569(3) | 12.570(3) | 20.243(4) |
| ***c*/Å** | 13.561(3) | 13.523(3) | 31.359(6) |
| ***α*/°** | 101.43(3) | 101.43(3) | - |
| ***β*/°** | 109.82(3) | 109.71(3) | 102.23(3) |
| ***γ*/°** | 99.23(3) | 99.18(3) | - |
| **Volume/Å³** | 1848.1(8) | 1822.1(7) | 8702(3) |
| **Z** | 2 | 2 | 1 |
| **Refs. collected** | 37092 | 37561 | 70936 |
| **Independent refs.** | 7306 | 7247 | 19926 |
| **$R_{int}$** | 0.0548 | 0.0415 | 0.1353 |
| **GooF** | 1.084 | 1.092 | 0.998 |
| **$R_1$ [I>=2σ (I)/all data]** | 0.0342/0.0370 | 0.0306/0.0311 | 0.0626/0.1282 |
| **$wR_2$ [I>=2σ (I)/all data]** | 0.0941/0.0954 | 0.0854/0.0857 | 0.1335/0.1641 |
| **Diffractometer** | MX1, Australian Synchrotron | MX1, Australian Synchrotron | MX1, Australian Synchrotron |

**Table S2.** Crystallographic and refinement parameters for **2Tb**, **2Yb**, and **3**.

## 2. Tables of Selected Bond Lengths

| | 1Eu | 1Dy | 1Ho | 1Er | 1Yb |
|---|---|---|---|---|---|
| **Ln1-O1** | 2.342(2) | 2.313(5) | 2.2848(15) | 2.287(2) | 2.275(5) |
| **Ln1-O2** | 2.336(2) | 2.271(6) | 2.2961(14) | 2.292(3) | 2.287(6) |
| **Ln1-O3** | 2.326(2) | 2.317(5) | 2.2774(14) | 2.279(3) | 2.271(6) |
| **Ln1-O4** | 2.330(3) | 2.304(6) | 2.2947(14) | 2.264(3) | 2.239(6) |
| **Ln1-N1** | 2.609(3) | 2.545(7) | 2.5311(17) | 2.562(3) | 2.501(5) |
| **Ln1-N2** | 2.633(3) | 2.590(7) | 2.5719(17) | 2.537(3) | 2.512(5) |
| **Ln1-N3** | 2.598(3) | 2.568(7) | 2.5369(17) | 2.534(3) | 2.502(5) |
| **Ln1-N4** | 2.604(3) | 2.550(7) | 2.5471(16) | 2.534(3) | 2.522(5) |
| **Ln2-O5** | 2.346(2) | 2.291(6) | 2.2958(13) | 2.293(2) | 2.240(7) |
| **Ln2-O6** | 2.346(2) | 2.297(6) | 2.2693(14) | 2.291(2) | 2.233(7) |
| **Ln2-O7** | 2.333(3) | 2.304(6) | 2.2912(14) | 2.286(2) | 2.253(6) |
| **Ln2-O8** | 2.314(2) | 2.299(6) | 2.2920(13) | 2.273(2) | 2.278(7) |
| **Ln2-N5** | 2.588(3) | 2.556(7) | 2.5223(16) | 2.537(3) | 2.510(7) |
| **Ln2-N6** | 2.600(3) | 2.569(7) | 2.5715(17) | 2.523(3) | 2.523(8) |
| **Ln2-N7** | 2.600(3) | 2.582(7) | 2.5432(17) | 2.543(3) | 2.541(8) |
| **Ln2-N8** | 2.633(3) | 2.564(8) | 2.5433(17) | 2.557(3) | 2.498(8) |

**Table S1.** Bond lengths around the lanthanoid metal in the **1Ln** series of compounds.

| | **$[Tb_2Mn(QCl)_8]$** | **$[Yb_2Mn(QCl)_8]$** |
|---|---|---|
| **Ln-N1** | 2.550(3) | 2.493(4) |
| **Ln-N2** | 2.554(3) | 2.509(3) |
| **Ln-N3** | 2.522(3) | 2.457(3) |
| **Ln-N4** | 2.541(3) | 2.483(3) |
| **Ln-O1** | 2.344(3) | 2.303(3) |
| **Ln-O2** | 2.320(3) | 2.264(3) |
| **Ln-O3*** | 2.275(3) | 2.223(3) |
| **Ln-O4** | 2.366(3) | 2.316(3) |
| **Mn-O1** | 2.203(3) | 2.204(3) |
| **Mn-O2** | 2.119(3) | 2.129(3) |
| **Mn-O4** | 2.185(3) | 2.180(3) |

**Table S2.** Bond lengths in the **2Ln** series of compounds, * denotes the terminal ligand which has a shorter Ln-O bond.

## 3. Magnetic Plots

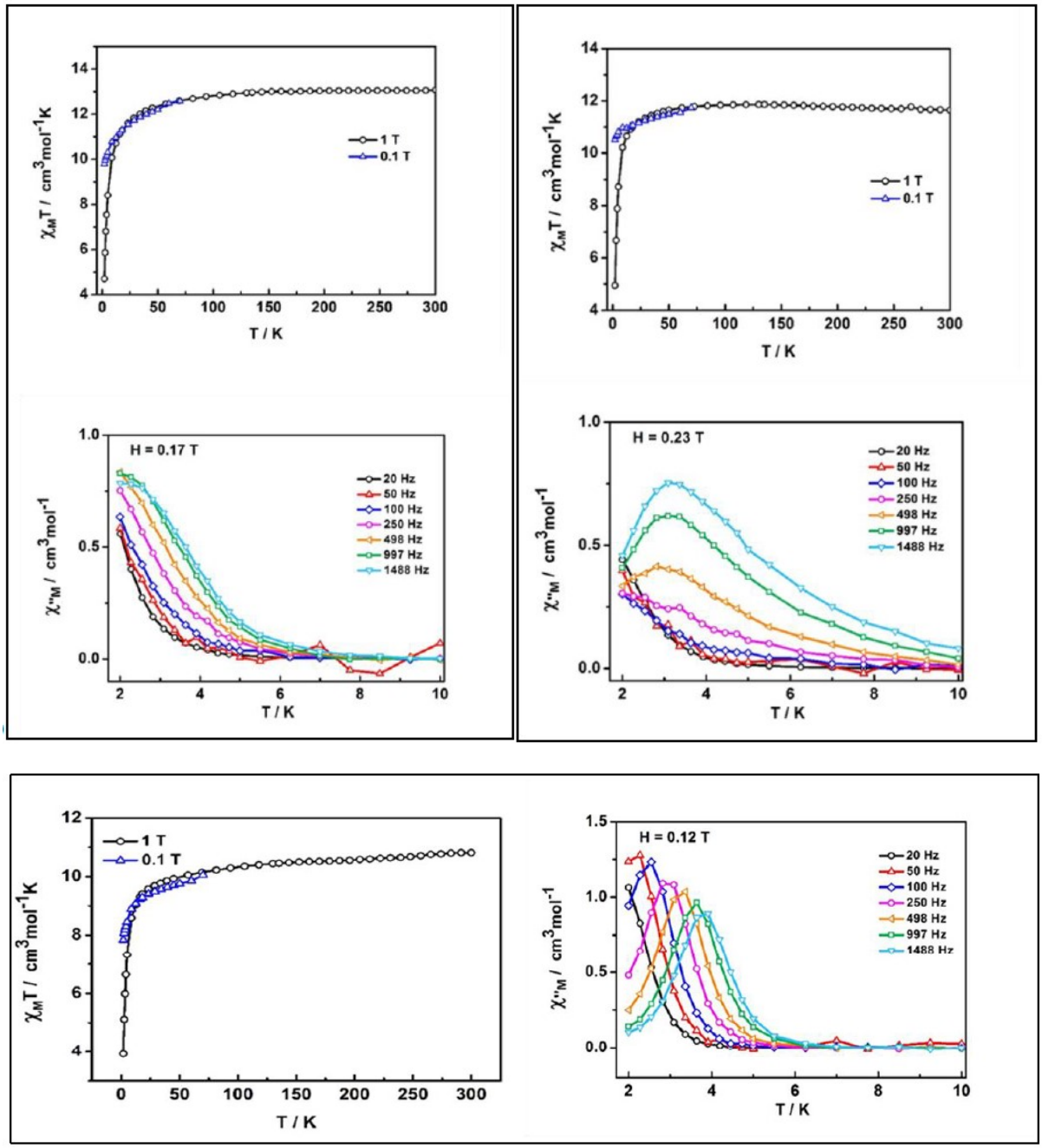


**Figure S1.** Plots of the static DC magnetic $\chi_M T$ vs. $T$ measurements and dynamic AC out-of-phase $\chi_M''$ vs. $T$ measurements for **1Dy** (top left), **1Tb** (top right), and **1Er** (bottom).

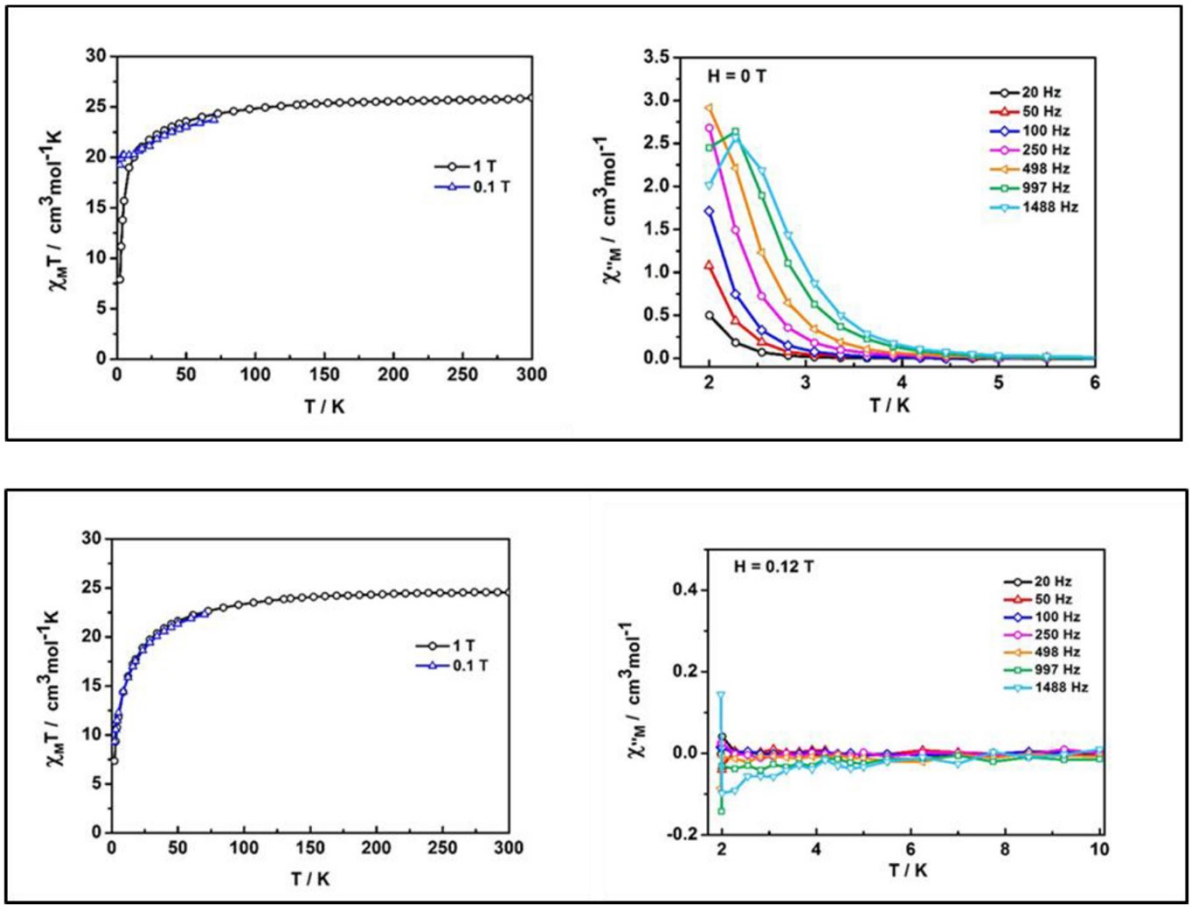


**Figure S2.** Magnetic measurements for **2Tb** (top) and **2Er** (bottom) showing $\chi_M T$ *vs*. temperature in fields of 1 T and 0.1 T and out-of-phase AC susceptibilities as a function of temperature at the frequencies listed in zero and 0.12 T DC fields, respectively.

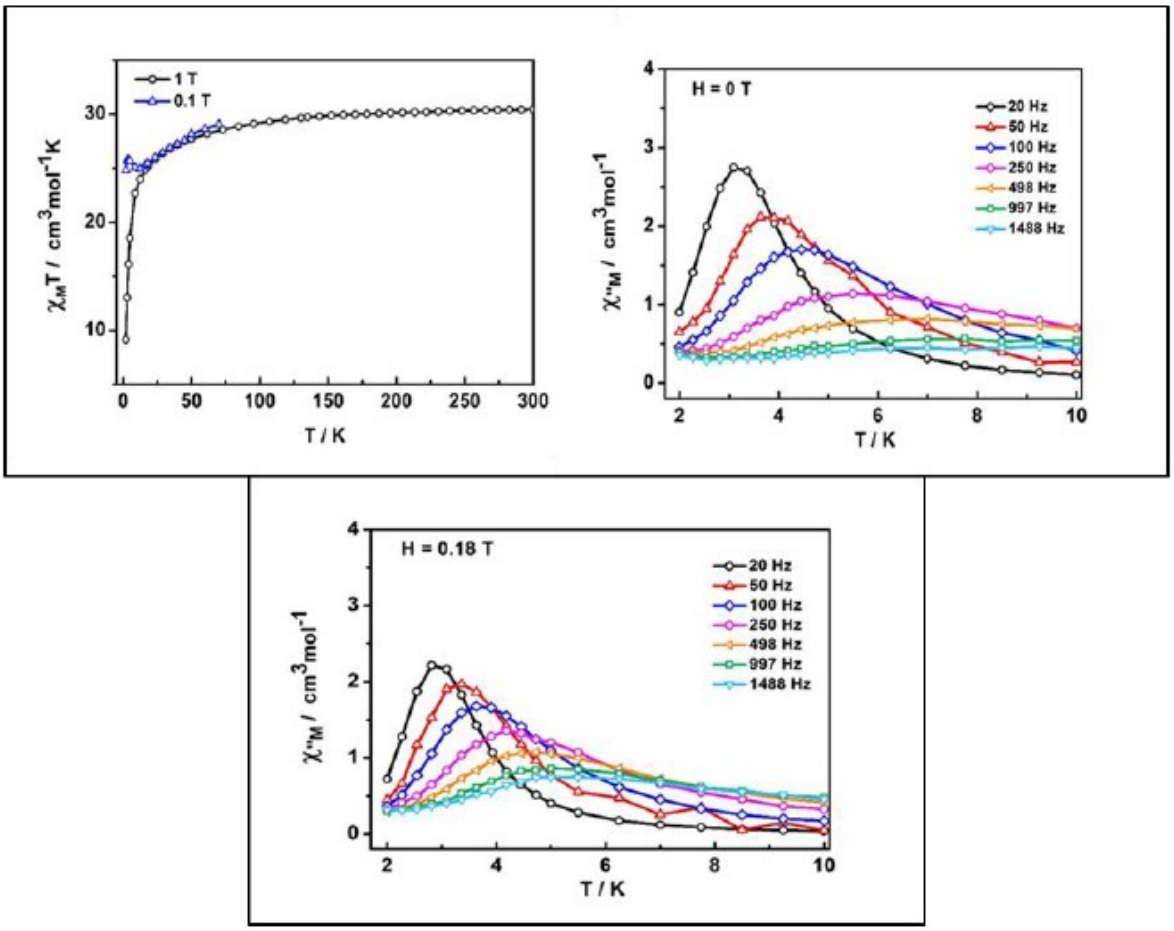


**Figure S3.** Magnetic measurements of **2Dy** showing $\chi_M T$ *vs.* temperature in fields of 1 T and 0.1 T (top left), and out-of-phase AC susceptibilities as a function of temperature at the frequencies listed in a zero DC field (top right) and at 0.18 T (bottom).

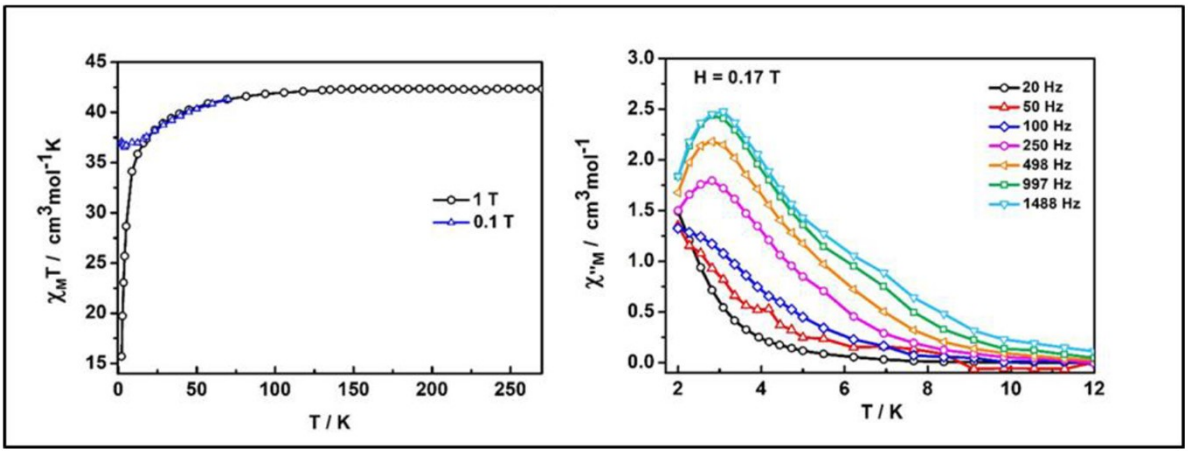


**Figure S4.** Plots of the static DC magnetic $\chi_M T$ vs. $T$ measurements and dynamic out-of-phase AC out-of-phase $\chi_M''$ vs. $T$ measurements for **3Dy**.

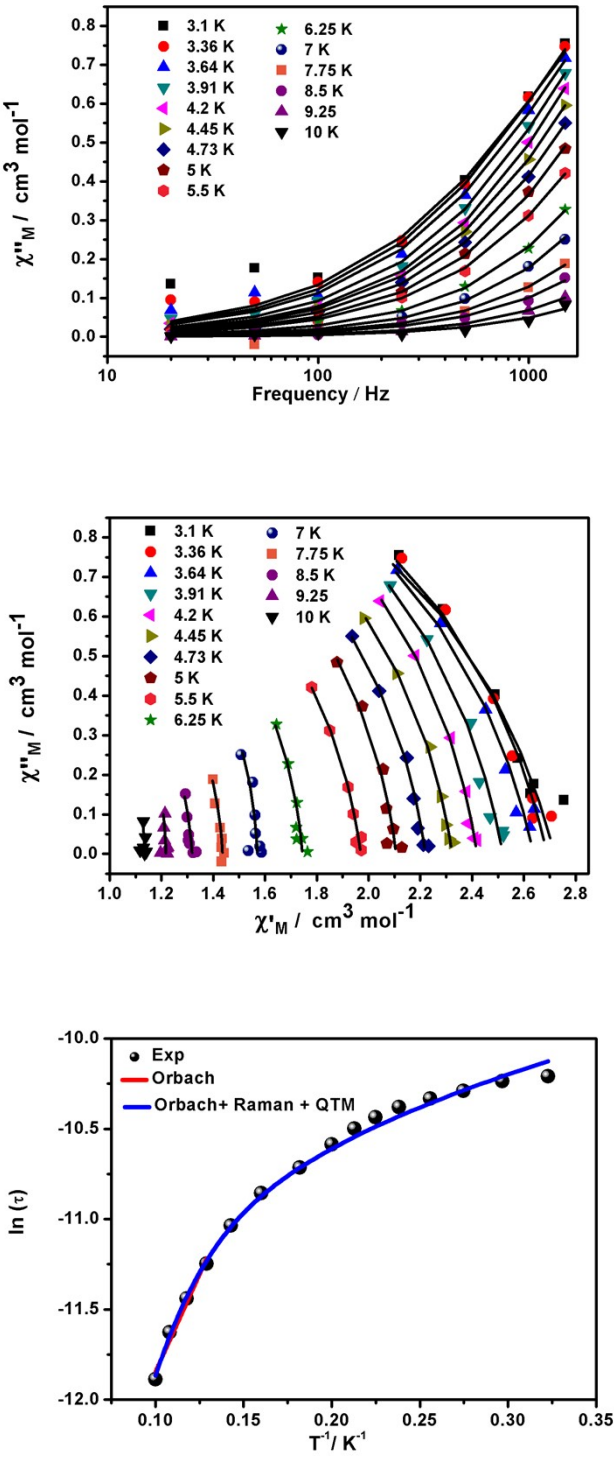


**Figure S5.** (top) $X_M''$ vs. frequency plots for **1Tb** with solid lines representing fitted data extracted from the CC-FIT program; (middle) Cole-Cole plots and fit (see main manuscript) for **1Tb**; (bottom) plot of ln(τ) vs. $T^{-1}$ for **1Tb** with experimental points as circles, the blue line fitted using Orbach plus Raman plus QTM, and the red line fitted using an Orbach mechanism of relaxation.

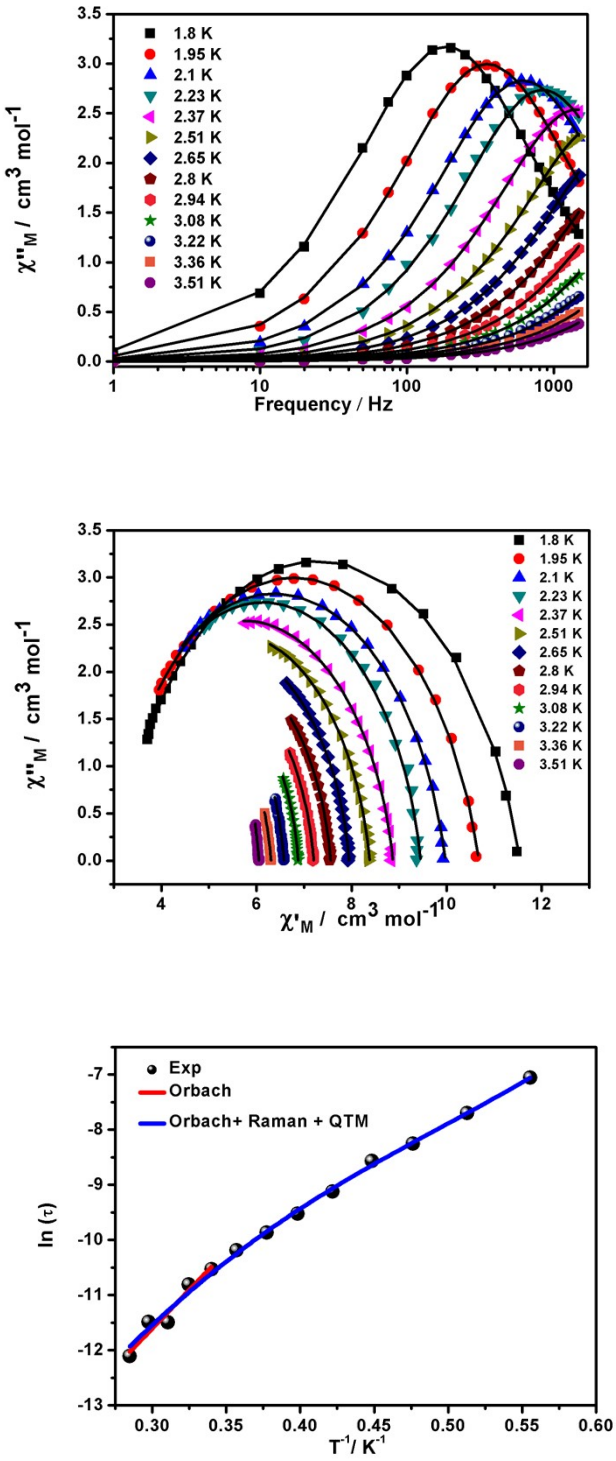


**Figure S6.** (top) $X_M''$ vs. frequency plots for **2Tb** with solid lines representing fitted data extracted from the CC-FIT program; (bottom) Cole-Cole plots and fit (see main manuscript) for **2Tb**; (bottom) plot of ln($\tau$) vs $T^{-1}$ for **2Tb** with experimental points as circles, the blue line fitted using Orbach plus Raman plus QTM, and the red line fitted using an Orbach mechanism of relaxation.

## 4. PXRD Data

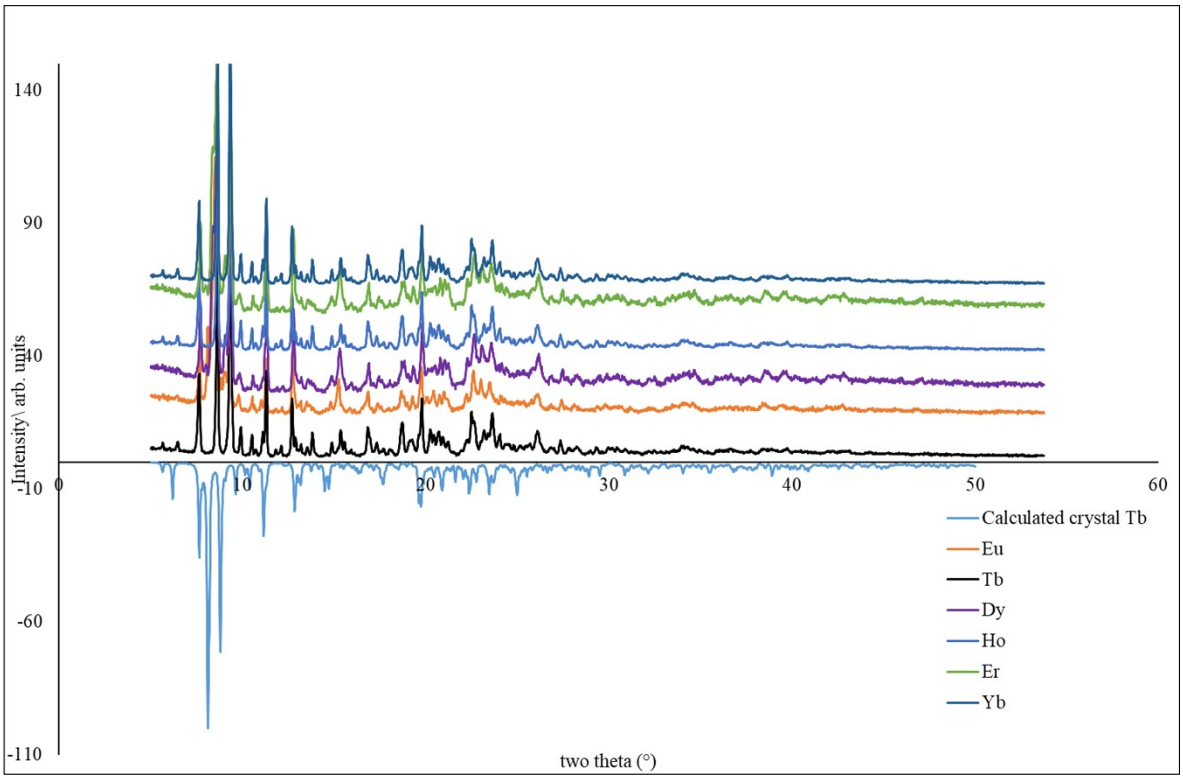


**Figure S7.** Comparison of the calculated PXRD pattern of **1Tb** (inverted) with the experimental PXRD patterns of all members of the **1Ln** series, demonstrating that all compounds are pure and isostructural.

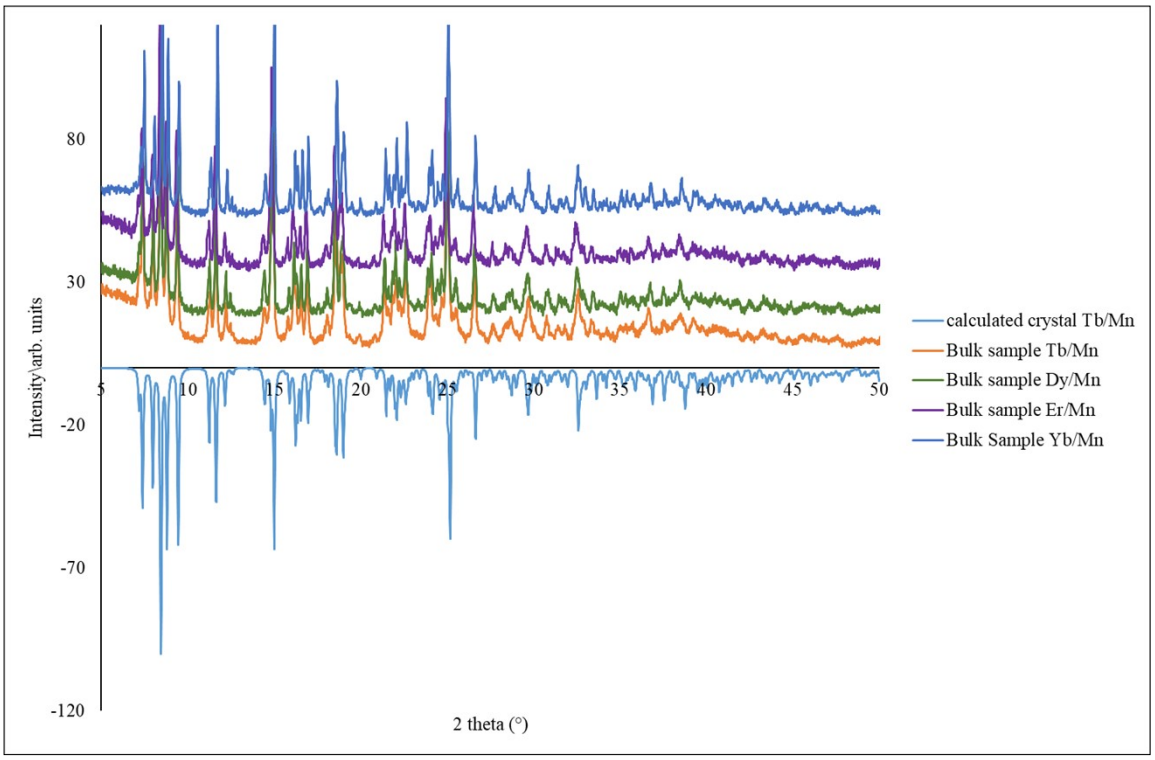


**Figure S8.** Comparison of the calculated PXRD pattern of **2Tb** (inverted) with the experimental PXRD patterns of all members of the **2Ln** series, demonstrating that all compounds are pure and isostructural.

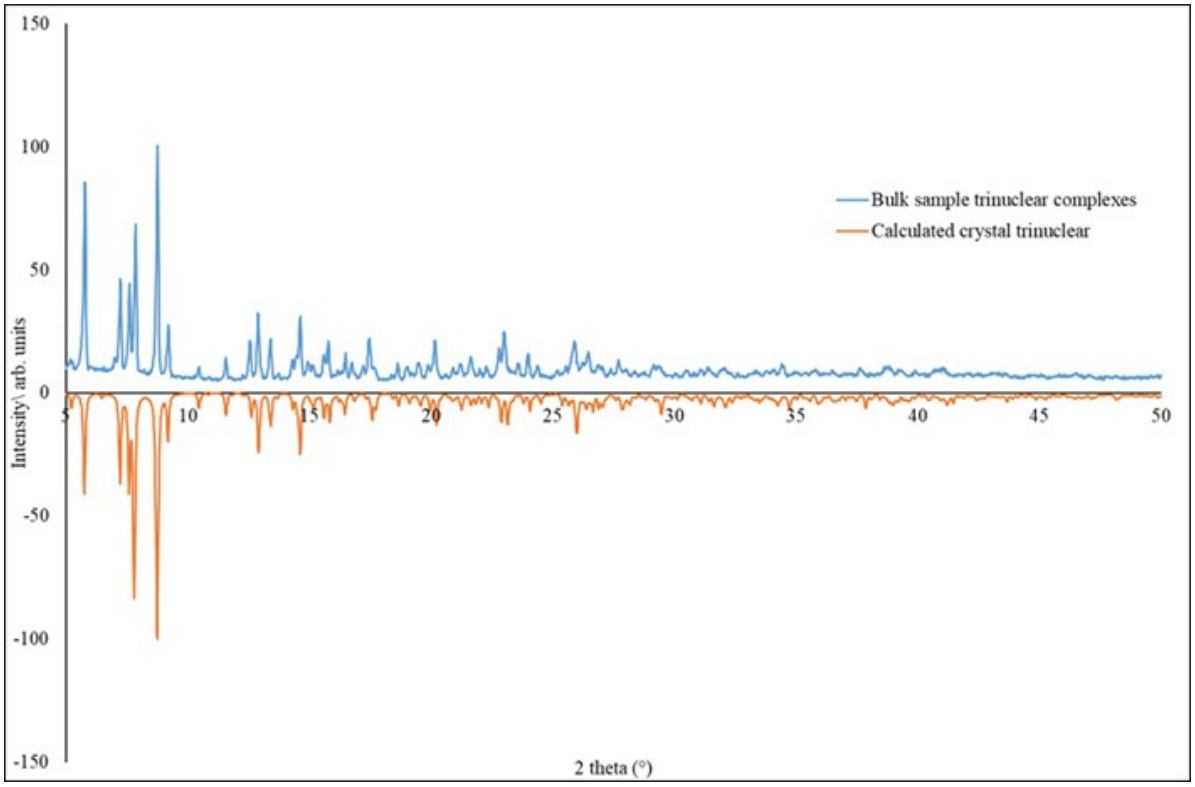


**Figure S9.** Comparison of the calculated PXRD pattern of **3** (inverted) with the experimental PXRD pattern.